

Thermodynamic Analysis of the Effect of Cholesterol on Dipalmitoylphosphatidylcholine Lipid Membranes

W. F. Drew Bennett, Justin L. MacCallum,[†] and D. Peter Tieleman*

Department of Biological Sciences, University of Calgary, 2500 University Drive NW, Calgary, Alberta T2N 1N4, Canada

Received October 30, 2008; E-mail: tieleman@ucalgary.ca

Abstract: Cholesterol is an important component of eukaryotic cellular membranes. Despite extensive literature on the physicochemical effects of cholesterol on membranes, much remains unknown about the precise role of cholesterol and its molecular interactions in membranes. Regular thermal fluctuations of lipids normal to the plane of the membrane are biologically relevant for many processes, such as interactions with enzymes, elastic properties, and hydrophobic matching, while larger fluctuations are involved in vesicle budding and fusion, passive lipid flip-flop, and pore formation. Here we used molecular dynamics simulations to investigate the thermodynamic effect of the cholesterol concentration on dipalmitoylphosphatidylcholine (DPPC) bilayers. We calculated the potentials of mean force for DPPC partitioning in DPPC bilayers containing 20 and 40 mol % cholesterol. Increasing the cholesterol content increases the free energy barrier for transferring the headgroup of DPPC to the center of the bilayer and slows the rate of DPPC flip-flop by orders of magnitude. Cholesterol increases the order, thickness, and rigidity of the bilayers, which restricts bilayer deformations and prevents pore formation. While DPPC flip-flop is pore-mediated in a pure bilayer, we do not observe pores in the 20 and 40 mol % bilayers. Increasing the cholesterol concentration causes a decrease in the free energy to transfer DPPC from its equilibrium position into bulk water—indicating that DPPC prefers to be in cholesterol-free bilayers. We also observe a reduction in small fluctuations of DPPC normal to the bilayer as the cholesterol concentration is increased.

Introduction

Cellular membranes are heterogeneous lipid bilayers that function primarily to separate aqueous cellular compartments and to act as scaffolds for membrane proteins. Although all membranes share the global function of acting as barriers between cellular environments, there exists great variability in the local composition and organization of membranes and their specific biophysical properties. Lipid composition varies between species, cell types, organelles, and even leaflets of the same membrane. For example, mammalian plasma membranes contain high concentrations of cholesterol (25–40 mol %), while their endoplasmic reticulum (ER) membranes have low cholesterol concentrations (0–5 mol %).¹

Thermal fluctuations of individual lipids from equilibrium, normal to the plane of the bilayer, are important in a number of biological processes. Interacting with transmembrane proteins and peptides induces hydrophobic matching of the lipids; lipids may lengthen to shield long hydrophobic transmembrane proteins from water or shorten to accommodate hydrophilic peptides or helices, such as antimicrobial peptides.² Protrusions of lipids from the bilayer are necessary for interaction with enzymes, such as phospholipases,³ as well as an initial step in vesicle fusion.^{4,5}

Individual lipids undergo intramembrane lipid exchange, or flip-flop, which involves a lipid translocating from one bilayer leaflet to the other. Most phosphatidylcholine (PC) lipids are synthesized in the ER on the cytoplasmic side, so flip-flop is necessary for them to reach the extracellular side of the plasma membrane.⁶ Dipalmitoylphosphatidylcholine (DPPC) flip-flop involves exposing the bulky, zwitterionic headgroup of the lipid to the hydrophobic interior of the bilayer. The time scale for PC exchange has been estimated experimentally between 1 and 90 h.^{7–9} The large discrepancy is due to differences in experimental conditions and methods. Efficient trafficking requires energy-dependent and energy-independent lipid flippases due to the slow rates for lipid flip-flop. In addition to lipid flippases (extracellular to intracellular), there are speculated floppases (intracellular to extracellular) and scramblases (both directions).⁶ As well, it has been shown that certain integral membrane proteins and model peptides can increase the rate of flip-flop in an energy-independent fashion.¹⁰ The existence of

[†] Present address: Department of Pharmaceutical Chemistry, University of California, San Francisco.

(1) Sprong, H.; van der Sluijs, P.; van Meer, G. *Nat. Rev. Mol. Cell Biol.* **2001**, *2*, 504–513.
 (2) Epanand, R. M.; Vogel, H. J. *Biochim. Biophys. Acta* **1999**, *1462*, 11–28.

(3) Berg, O. G.; Gelb, M. H.; Tsai, M. D.; Jain, M. K. *Chem. Rev.* **2001**, *101*, 2613–2653.

(4) Marrink, S. J.; Mark, A. E. *J. Am. Chem. Soc.* **2003**, *125*, 11144–5.

(5) Stevens, M. J.; Hoh, J. H.; Woolf, T. B. *Phys. Rev. Lett.* **2003**, *91*, 188102.

(6) Daleke, D. L. *J. Lipid Res.* **2003**, *44*, 233–42.

(7) De Kruijff, B.; Van Zoelen, E. J. *Biochim. Biophys. Acta* **1978**, *511*, 105–15.

(8) Kornberg, R. D.; McConnell, H. M. *Biochemistry* **1971**, *10*, 1111–20.

(9) Wimley, W. C.; Thompson, T. E. *Biochemistry* **1990**, *29*, 1296–1303.

(10) Kol, M. A.; van Laak, A. N. C.; Rijkers, D. T. S.; Killian, J. A.; de Kroon, A. I. P. M.; de Kruijff, B. *Biochemistry* **2003**, *42*, 231–237.

the complex system of proteins, which control the distribution of lipids throughout cells, suggests passive flip-flop is a natural process cells must overcome. The ER membrane contains a symmetric distribution of lipids, while the plasma membrane has an asymmetric distribution, with PC and sphingomyelin enriched in the extracellular leaflet and phosphatidylserine (PS) and phosphatidylethanolamine (PE) in the inner leaflet. Disruption of the asymmetry and exposure of PS to the extracellular leaflet can signal apoptosis.⁶

Cholesterol is known to be important for modulating membrane fluidity; it broadens the transition of bilayers from the gel phase to the liquid crystalline phase and creates an intermediate liquid-ordered phase.¹¹ In the liquid-ordered phase, cholesterol increases the packing of phospholipids and their orientational order, increases the thickness of the hydrophobic portion of the bilayer, and decreases the rate of motion of the lipid tails.¹² The bilayer bending¹³ and area compressibility¹⁴ moduli both increase as the concentration of cholesterol increases—indicating stiffening of the bilayer. The molecular basis for the condensing effect of cholesterol on lipid bilayers remains poorly understood. Evidence has shown that similar sterol molecules do not have the same condensing effect on lipid bilayers compared to cholesterol.^{15–17} This suggests cholesterol is a highly specialized molecule with a precise structure.

Early theoretical studies using simplified models reproduced qualitative effects of cholesterol on bilayers.¹⁸ Recently, there have been fully solvated atomistic simulations of cholesterol in bilayers on a 10–100 ns time scale. Systematic simulations of cholesterol from 0 to 40 mol % in DPPC bilayers showed that many of the effects of cholesterol, such as ordering the DPPC chains, reducing the area per lipid, and increasing the area compressibility, agreed with the experimental data.¹⁹ Important membrane properties, such as lateral pressure profiles and bending moduli, have been calculated for DPPC bilayers containing cholesterol²⁰ and for raftlike bilayers.²¹ Several groups have simulated ternary mixtures of cholesterol, sphingomyelin, and phosphatidylcholine to investigate the behavior of putative lipid rafts.^{21–23} Zhang and co-workers determined the free energy for cholesterol desorption from a palmitoylphosphatidylcholine (POPC) and a sphingomyelin bilayer and showed cholesterol had a greater affinity for sphingomyelin.²⁴

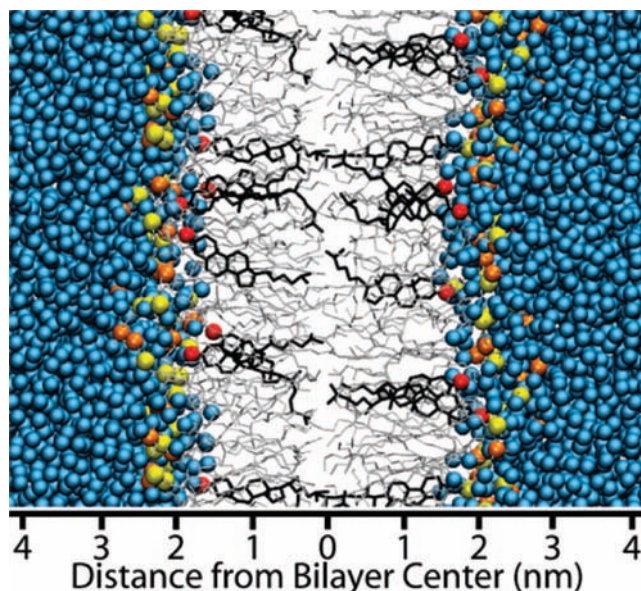


Figure 1. Snapshot of a representative 20% cholesterol bilayer. Water is represented as blue spheres. The phosphorus and nitrogen of DPPC are shown as yellow and orange spheres, respectively. The oxygen in cholesterol is shown as red spheres. DPPC is shown as thin gray lines, and cholesterol is shown as thin black lines.

Computer simulations have been used to investigate the molecular mechanism of lipid flip-flop at a resolution that is difficult to reach by experimental techniques. Using preformed pores, it was shown that multiple DMPC molecules flip-flop across a hydrophilic pore on a 60 ns time scale.²⁵ Pore-mediated flip-flop was also observed for DPPC in a pure DPPC membrane.²⁶ The mechanism of flip-flop for other lipids with less bulky and charged head groups, such as sterols, remains unknown. The fast rate of cholesterol flip-flop determined from experiment (half-time of <math>< 1\text{ s}</math>) suggests it is not pore mediated.²⁷ It was shown that a derivative of cholesterol with a ketone headgroup flip-flopped on the nanosecond time scale without water pore formation.²⁸

Here we investigate cholesterol's effect on the thermodynamics of DPPC movement normal to the bilayer. Previously, Tieleman and Marrink calculated the potential of mean force (PMF) for the transfer of a DPPC lipid through a pure DPPC bilayer.²⁶ Many important membrane properties were estimated from the PMF, such as the critical micelle concentration, the rate for DPPC flip-flop, and the permeation rates for ions and water—all of which compare well to the experimental data. We present PMFs for DPPC partitioning in 20 and 40 mol % cholesterol bilayers. From these PMFs, we show that cholesterol has a concentration-dependent effect on the movement of DPPC normal to the bilayer. The mechanism of spontaneous DPPC flip-flop changes upon inclusion of cholesterol in the bilayer, and the rate of flip-flop decreases by orders of magnitude. Desorbing DPPC from cholesterol-rich bilayers is easier than

(11) McMullen, T. P. W.; Lewis, R. N. A. H.; McElhaney, R. N. *Curr. Opin. Colloid Interface Sci.* **2004**, *8*, 459–468.

(12) Holthuis, J. C. M.; van Meer, G.; Huitema, K. *Mol. Membr. Biol.* **2003**, *20*, 231–241.

(13) Evans, E.; Rawicz, W. *Phys. Rev. Lett.* **1990**, *64*, 2094–2097.

(14) Needham, D.; McIntosh, T. J.; Evans, E. *Biochemistry* **1988**, *27*, 4668–73.

(15) Arora, A.; Raghuraman, H.; Chattopadhyay, A. *Biochem. Biophys. Res. Commun.* **2004**, *318*, 920–6.

(16) Rog, T.; Pasenkiewicz-Gierula, M.; Vattulainen, I.; Karttunen, M. *Biophys. J.* **2007**, *92*, 3346–57.

(17) Vainio, S.; Jansen, M.; Koivusalo, M.; Rog, T.; Karttunen, M.; Vattulainen, I.; Ikonen, E. *J. Biol. Chem.* **2006**, *281*, 348–55.

(18) Scott, H. L. *Biophys. J.* **1991**, *59*, 445–455.

(19) Hofsass, C.; Lindahl, E.; Edholm, O. *Biophys. J.* **2003**, *84*, 2192–2206.

(20) Patra, M. *Eur. Biophys. J.* **2005**, *35*, 79–88.

(21) Niemela, P. S.; Ollila, S.; Hyvonen, M. T.; Karttunen, M.; Vattulainen, I. *PLoS Comput. Biol.* **2007**, *3*, 304–312.

(22) Zhang, Z.; Bhide, S. Y.; Berkowitz, M. L. *J. Phys. Chem. B* **2007**, *111*, 12888–97.

(23) Pandit, S. A.; Jakobsson, E.; Scott, H. L. *Biophys. J.* **2004**, *87*, 3312–22.

(24) Zhang, Z.; Lu, L.; Berkowitz, M. L. *J. Phys. Chem. B* **2008**, *112*, 3807–11.

(25) Gurtovenko, A. A.; Vattulainen, I. *J. Phys. Chem. B* **2007**, *111*, 13554–9.

(26) Tieleman, D. P.; Marrink, S. J. *J. Am. Chem. Soc.* **2006**, *128*, 12462–12467.

(27) Steck, T. L.; Ye, J.; Lange, Y. *Biophys. J.* **2002**, *83*, 2118–2125.

(28) Rog, T.; Stimson, L. M.; Pasenkiewicz-Gierula, M.; Vattulainen, I.; Karttunen, M. *J. Phys. Chem. B* **2008**, *112*, 1946–52.

from pure DPPC bilayers, indicating DPPC prefers bilayers with a low cholesterol content.

Methods

The simulation system consists of 64 lipids and ~ 3000 water molecules. For the 20 mol % cholesterol 12 DPPC lipids were replaced by cholesterol molecules; for the 40 mol % cholesterol 26 DPPC lipids were replaced by cholesterol molecules. The same simulation setup was previously used in the calculation of the DPPC PMF in a pure DPPC bilayer (64 lipids).²⁶ Figure 1 shows a representative snapshot of the 20 mol % cholesterol bilayer system during equilibration.

All simulations were performed with the GROMACS 3.3.1 software package.^{29,30} DPPC was modeled with the Berger et al. force field parameters.³¹ Water was represented by the simple point charge model.³² The force field for cholesterol was based on the GROMOS force field, with minor changes.³³ Lennard-Jones and electrostatic interactions were cut off at 0.9 nm. The smooth particle mesh Ewald method was used to evaluate long-range electrostatic interactions.^{34,35} Bond lengths were constrained with the LINCS algorithm³⁶ for DPPC and cholesterol and with the SETTLE algorithm³⁷ for water—allowing a 2 fs time step. The temperatures of water, DPPC, and cholesterol were kept constant separately at 323 K using the weak coupling algorithm with a 0.1 ps coupling constant.³⁸ Semi-isotropic pressure coupling was used with a 2.5 ps. coupling constant. The pressures normal and lateral to the bilayer plane were separately maintained at 1 bar. The 20 and 40 mol % cholesterol bilayers were constructed from a 64-lipid pure DPPC bilayer²⁶ by replacing random DPPC molecules with cholesterol. Both bilayers were equilibrated for 50 ns.

Umbrella sampling was used to calculate the potential of mean force acting on the phosphate group of DPPC as a function of the distance from the center of the bilayer. Two DPPC molecules were restrained, with one on each side of the bilayer. The molecules were staggered, such that when one is in bulk water, the other is at the center of the bilayer. Staggering the two molecules in this way ensures that they are always at least 5 nm from each other. We have previously shown that having two positively charged smaller molecules staggered 3.7 nm apart causes little change compared to calculations where a single molecule was restrained.³⁹ However, restraining two molecules instead of one allows twice as much data to be collected at no additional computational cost. The distance between the center of the bilayer and the phosphate groups of the staggered DPPC molecules was restrained using a series of harmonic potentials with a force constant of $3000 \text{ kJ mol}^{-1} \text{ nm}^{-2}$. A total of 51 simulation windows were used to transfer one lipid from bulk water to the center of the bilayer and the other lipid from the center of the bilayer to bulk water with 0.1 nm between adjacent windows. We used the weighted histogram analysis method⁴⁰ to calculate the potential of mean force. The standard

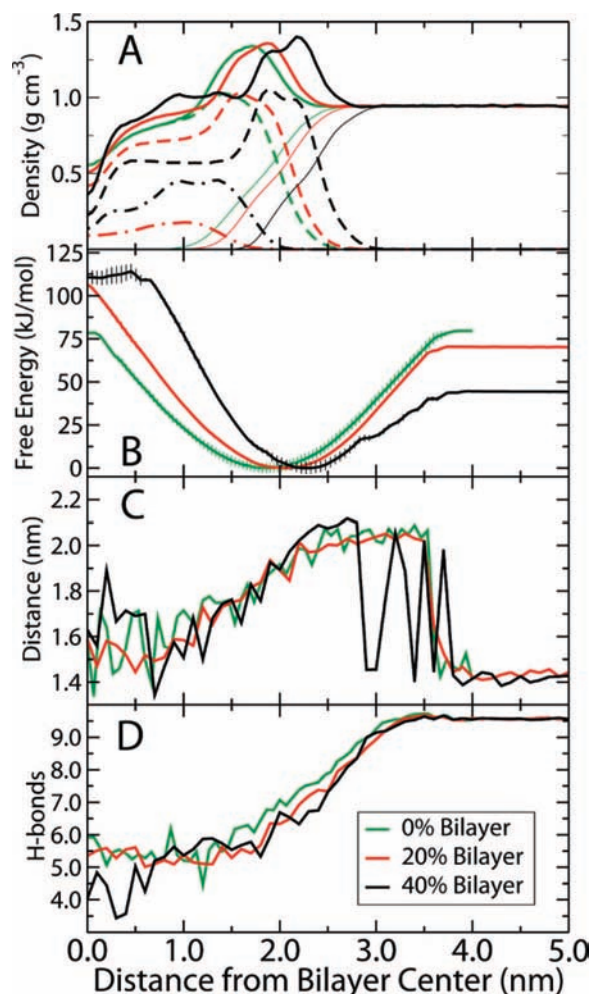


Figure 2. (A) Partial density profiles of the 0%, 20%, and 40% bilayers. The total system density is denoted by solid thick lines, the water density is denoted by solid thin lines, the DPPC density is denoted by dashed lines, and the cholesterol density is denoted by dotted-dashed lines. (B) PMFs for a DPPC partitioning through the 0%,²⁶ 20%, and 40% bilayers. The PMFs were set equal to zero at the equilibrium position of DPPC in the respective bilayer. Error bars are the standard errors from the two leaflets' PMFs. (C) Average number of hydrogen bonds to the DPPC of interest. We use a geometric definition of a hydrogen bond with a distance cutoff of 0.35 nm and an angle cutoff of 30° between acceptors and donors. (D) Average distance between the phosphate and the *sn*-2 tail of the DPPC of interest.

error was estimated on the basis of the asymmetry between the PMFs for the two lipids on either side of the bilayer. Each window in the 20% cholesterol bilayer was run for 50 ns, while the 40% cholesterol bilayer windows were run for 80 ns each. We judged PMF convergence on the standard error of the two leaflets' independent PMFs. We extended the 40% cholesterol simulations to 80 ns to attain better sampling of the rough curve for desorption (see the Results).

Results

For brevity, the systems will be referred to by their approximate concentration (mol %) of cholesterol; i.e., the DPPC bilayer containing ~ 20 mol % cholesterol will be referred to as the 20% bilayer. Figure 2A shows partial density distributions of the 0%, 20%, and 40% bilayers. Consistent with many simulations¹⁹ and experiments,⁴¹ as the concentration of cholesterol is increased, the overall thickness of the bilayer increases.

(29) Berendsen, H. J. C.; Vanderveen, D.; Vandrunen, R. *Comput. Phys. Commun.* **1995**, *91*, 43–56.

(30) Lindahl, E.; Hess, B.; van der Spoel, D. *J. Mol. Model.* **2001**, *7*, 306–317.

(31) Berger, O.; Edholm, O.; Jahnig, F. *Biophys. J.* **1997**, *72*, 2002–2013.

(32) Berendsen, H. J. C.; Postma, J. P. M.; van Gunsteren, W. F.; Hermans, J. In *Intermolecular Forces*; Pullman, B., Ed.; D. Reidel: Dordrecht, The Netherlands, 1981; pp 331–342.

(33) Holtje, M.; Forster, T.; Brandt, B.; Engels, T.; von Rybinski, W.; Holtje, H. D. *Biochim. Biophys. Acta* **2001**, *1511*, 156–167.

(34) Essmann, U.; Perera, L.; Berkowitz, M. L.; Darden, T.; Lee, H.; Pedersen, L. G. *J. Chem. Phys.* **1995**, *103*, 8577–8593.

(35) Darden, T.; York, D.; Pedersen, L. *J. Chem. Phys.* **1993**, *98*, 10089–10092.

(36) Hess, B.; Bekker, H.; Berendsen, H. J. C.; Fraaije, J. G. E. M. *J. Comput. Chem.* **1997**, *18*, 1463–1472.

(37) Miyamoto, S.; Kollman, P. A. *J. Comput. Chem.* **1992**, *13*, 952–962.

(38) Berendsen, H. J. C.; Postma, J. P. M.; Vangunsteren, W. F.; Dinola, A.; Haak, J. R. *J. Chem. Phys.* **1984**, *81*, 3684–3690.

(39) Maccallum, J. L.; Bennett, W. F.; Tieleman, D. P. *Biophys. J.* **2008**, *94*, 3393–3404.

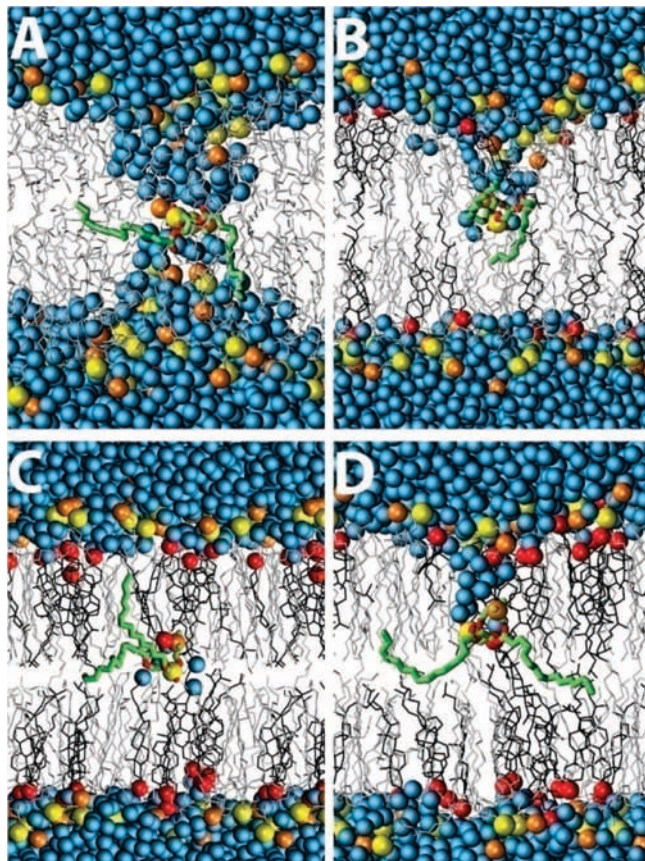


Figure 3. Snapshots of DPPC at various positions within the 20% and 40% bilayers. The molecular representations are the same as in Figure 1, except the restrained DPPC is denoted with thick green lines. (A) Phosphate of DPPC at the center of the 0% bilayer. A large pore spanning both bilayer leaflets forms. (B) Phosphate of DPPC at the center of the 20% bilayer. A water defect forms to solvate DPPC's charged headgroup. (C) Phosphate of DPPC at the center of the 40% bilayer. Four or five water molecules and an inverted cholesterol are pulled into the bilayer to solvate DPPC's headgroup. (D) Phosphate of DPPC at 0.5 nm from the center of the 40% bilayer. A water defect forms to solvate the charged headgroup of DPPC.

In Figure 2B we show PMFs for a DPPC lipid partitioning in the 0%,²⁶ 20%, and 40% bilayers. During umbrella sampling, we restrained the phosphate of DPPC, so all distances mentioned throughout refer to the position of the phosphate. The PMFs for all three bilayers have deep free energy minima at the equilibrium position of DPPC in the bilayer. As the concentration of cholesterol is increased, the position of the free energy trough moves farther from the bilayer center, consistent with the increase in bilayer thickness. There is a large free energy barrier for partitioning the phosphate to the bilayer center, which is the primary free energy barrier for flip-flop. The free energy barriers for flip-flop are 80, 106, and 111 kJ/mol for the 0%, 20%, and 40% bilayers, respectively. As well, there is a steep slope in the PMF as DPPC moves out of the bilayer into bulk water. For the 0%, 20%, and 40% bilayers, the free energies for desorption are 80, 70, and 44 kJ/mol.

The PMFs for the 0% and 20% bilayers share a similar shape; the slope to either side of the equilibrium position is symmetric, and the peak in free energy is at the bilayer center. This is in

contrast to the asymmetric shape of the PMF for the 40% bilayer. There is a large increase in free energy as the phosphate moves toward the center of the 40% bilayer, until the free energy plateaus at ~ 0.5 nm from the bilayer center. As the DPPC moves out of the 40% bilayer and into water, the free energy increases more slowly and the PMF is much rougher compared to those of the 0% and 20% bilayers. This region may suffer from poor sampling due to the slower dynamics of the tightly packed 40% bilayer.

The steep slope in the PMFs as we move DPPC into the hydrophobic core of the bilayer corresponds to large defects in the structure of the bilayer to prevent the desolvation of the charged lipid. For the 0% bilayer, when the phosphate of DPPC is at the center of the bilayer, there is a water pore spanning the entire bilayer (Figure 3A). When the phosphate of DPPC is at the center of the 20% bilayer, there is a single-sided water defect (Figure 3B). There is no water defect for the DPPC at the center of the 40% bilayer (Figure 3C); instead four or five water molecules and occasionally an inverted cholesterol are pulled into the hydrophobic core of the bilayer to solvate the headgroup of DPPC. Moving the phosphate of DPPC to ~ 0.5 nm from the center of the bilayer causes a water defect to form (Figure 3D). For each simulation window, we calculated the average number of hydrogen bonds to the restrained DPPC molecule (Figure 2D). Transferring the lipid from bulk water to the equilibrium position in the bilayer causes a decrease in the number of hydrogen bonds to the DPPC, from 9.5 in bulk water to 7 in the bilayer. For the 0% and 20% bilayers, the total number of hydrogen bonds to the DPPC remains nearly constant as the lipid is moved into the center of the bilayer, due to the formation of a large water defect (Figure 3B). The 40% bilayer has a decrease in the number of hydrogen bonds to the DPPC lipid near the bilayer center, which coincides with the plateau in the PMF and the dissipation of the water defect (Figure 3C,D).

Phospholipids are long and flexible molecules, which allows them to adopt different conformations in different environments, such in a bilayer and in bulk water. To quantify the relative compactness of DPPC, we calculated the average distance between the phosphate and the terminal methyl group of its *sn*-2 tail for each simulation window (Figure 2C). DPPC is most compact in bulk water; it has the shortest distance between the headgroup and the tail. The maximum distance is near the lipid equilibrium position, as the phosphate moves into bulk water. At the bilayer center, DPPC is quite compact, with only a slightly longer distance from headgroup to tail compared to that in bulk water. As the DPPC moves out of the 40% bilayer, there are large fluctuations in the distance between the headgroup and the tail, leading to the noise in Figure 2C (from 2.8 to 3.8 nm). Through this region, the DPPC fluctuates between having its tails folded up in bulk water (Figure 4A) and having its tails inserted in the bilayer (Figure 4B). We observe both conformations in single simulation windows, although exchange between them is slow. In contrast, for the 0% and 20% bilayers, there appears to be a critical distance at which the DPPC tails stop interacting with the bilayer (Figure 2C). To reduce the roughness of the 40% bilayer PMF in this region, we increased the sampling by running each umbrella window for 80 ns.

The broad troughs in the PMFs (Figure 2B) illustrate that at equilibrium individual lipids can move large distances normal to the membrane plane, with normal thermal fluctuations. As we increase the cholesterol content, the troughs of the PMFs narrow. The extent of thermal fluctuations normal to the bilayer

(40) Kumar, S.; Bouzida, D.; Swendsen, R. H.; Kollman, P. A.; Rosenberg, J. M. *J. Comput. Chem.* **1992**, *13*, 1011–1021.

(41) Hung, W. C.; Lee, M. T.; Chen, F. Y.; Huang, H. W. *Biophys. J.* **2007**, *92*, 3960–3967.

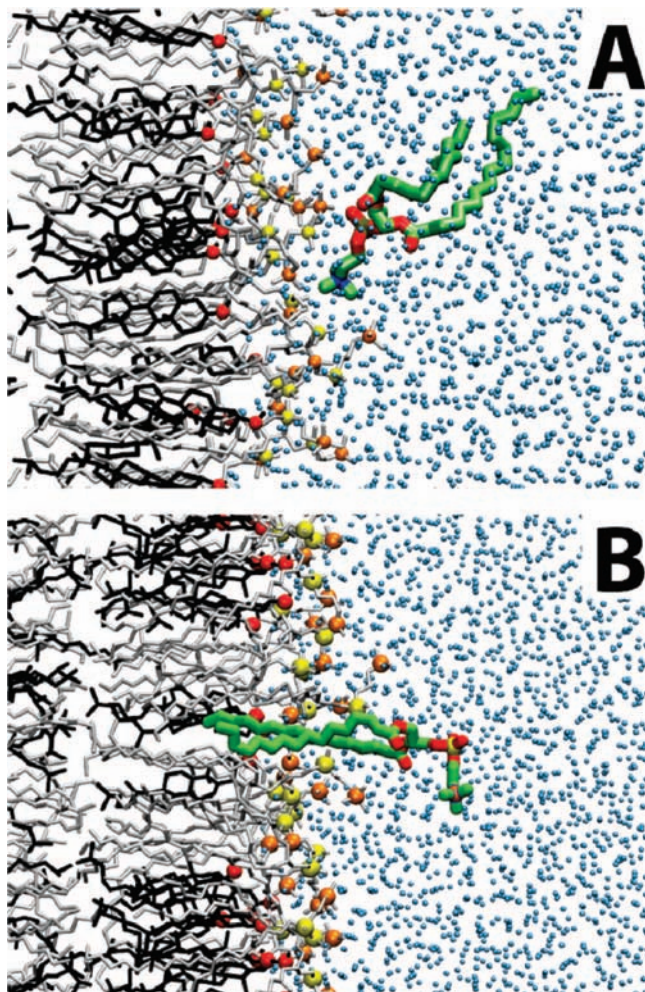


Figure 4. Snapshots of DPPC as it desorbs from the 20% and 40% bilayers. The representation of molecules is similar to that in Figure 3, except the water, phosphorus, nitrogen, and oxygen spheres are smaller. (A) The phosphate of DPPC is 2.9 nm from the 40% bilayer center; both acyl tails fold up in bulk water instead of interacting with the bilayer. (B) With 3.5 nm between the 40% bilayer center and the phosphate of DPPC, its tails insert into the bilayer.

has been determined by measuring the distance across the PMF troughs at a free energy of $2RT$. DPPC can move ~ 0.8 nm from equilibrium in the 0% and 20% bilayers, while only ~ 0.6 nm in the 40% bilayer, with $2RT$ of energy.

Discussion

Pores. The formation of transient water defects and pores in lipid membranes has important biological implications. The major energetic barrier for lipid flip-flop is likely the bulky, polar headgroup partitioning through the center of the hydrophobic tail region of the bilayer. To accommodate the charged molecule, the bilayer deforms to allow a lipid-lined water defect to keep the DPPC solvated. At the center of the 0% bilayer, the DPPC causes a water pore across the bilayer.²⁶ The free energy for pore formation in a DPPC bilayer was determined to be 80 kJ/mol. We did not observe pore formation when the phosphate of DPPC was at the center of the 20% or 40% bilayers. Therefore, we can speculate that the free energy for pore formation would be greater than 106 and 111 kJ/mol in the 20% and 40% bilayers. It would be much more difficult to form pores in cellular membranes with a high cholesterol content.

Experimental studies have shown that the permeation rate of polar molecules through bilayers decreases with increasing cholesterol concentration.⁴² As well, many recent simulations of polar and charged molecules in the acyl tail region of bilayers have observed similar defects, which are stable over long time scales (10–100 ns) and independent of the starting structure.^{26,39,43–45} The energetic cost of a water defect is due to deforming the structure of the bilayer and the cost of forming an interface between water and the lipid tails. Moving the charged molecule farther into the bilayer increases the cost of forming the water defect, which translates into a steep slope of the PMF. The defect dissipates once it becomes less expensive to have the charged molecule exposed to the low dielectric environment than to form the defect. We observe steeper slopes in the PMFs as we increase the cholesterol content. Cholesterol increases the order and rigidity of bilayers, which likely prevents defect formation. The 40% bilayer has a much steeper slope than the 20% bilayer, but at ~ 0.5 nm from the bilayer center the water defect dissipates. Once the water defect breaks, the PMF levels off until the bilayer center. Other simulations of polar molecules partitioning through bilayers have shown similar effects.⁴⁵

Our results have implications for all polar and charged molecules interacting with lipid bilayers. It has been shown that cationic penetrating peptides⁴⁶ and antimicrobial peptides⁴⁷ induce transient pore formation in bilayers. Therefore, membranes with high cholesterol, such as the plasma membrane, would have a greater barrier for pore formation than membranes with a low cholesterol content, such as the ER membrane.

Flip-Flop Rate. As discussed above, the mechanism of DPPC flip-flop differs among the three bilayers. In the 0% bilayer flip-flop is pore-mediated, so multiple lipids can flip simultaneously, along with other molecules, such as water and sodium ions.²⁶ At the center of the 20% bilayer, the headgroup of DPPC forms a single-sided water defect. We did not observe a membrane-spanning pore in any of our 20% bilayer simulations; however, we cannot rule out that possibility entirely, so the mechanism of transition of DPPC from the bilayer center to the opposite leaflet is uncertain. No pore is involved in DPPC flipping across the 40% bilayer; the headgroup of DPPC is surrounded by four or five waters and occasionally an inverted cholesterol at the center of the 40% bilayer.

The high free energy barriers for DPPC flip-flop agree qualitatively with the long rates that have been determined experimentally for this process.^{7–9} From the pure DPPC PMF, flip-flop was estimated to occur on a time scale of 4–30 h, which is well within the experimental range of rates.²⁶ The estimated rate relied upon the phosphate of DPPC forming a water pore at the bilayer center, which was assumed to be the transition state of the process.²⁶ The rate for the 0% bilayer was dependent on the rate of formation of the transition state, which was estimated using

(42) Simons, K.; Vaz, W. L. *Annu. Rev. Biophys. Biomol. Struct.* **2004**, *33*, 269–95.

(43) Dorairaj, S.; Allen, T. W. *Proc. Natl. Acad. Sci. U.S.A.* **2007**, *104*, 4943–4948.

(44) Freites, J. A.; Tobias, D. J.; von Heijne, G.; White, S. H. *Proc. Natl. Acad. Sci. U.S.A.* **2005**, *102*, 15059–64.

(45) MacCallum, J. L.; Bennett, W. F. D.; Tieleman, D. P. *J. Gen. Physiol.* **2007**, *129*, 371–7.

(46) Herce, H. D.; Garcia, A. E. *Proc. Natl. Acad. Sci. U.S.A.* **2007**, *104*, 20805–20810.

(47) Leontiadou, H.; Mark, A. E.; Marrink, S. J. *J. Am. Chem. Soc.* **2006**, *128*, 12156–61.

$$k_f/k_d = e^{-(\Delta G/RT)} \quad (1)$$

where k_f is the rate of formation of the transition state, k_d is the rate of pore dissipation, and ΔG is the free energy barrier.²⁶ We cannot make a direct estimate for the rate of flip-flop in the 20% and 40% bilayers because we are uncertain about the transition states, and even if we were certain, it would be nontrivial to make an accurate estimate of k_d . Pore dissipation has been estimated to occur on a 10–100 ns time scale, putting it at the limit of current computational feasibility.^{48,49} Using the same assumptions as in ref 26 and the same estimate for k_d (10^7 – 10^8 s⁻¹), we can make a crude estimate for the rate of flip-flop. Using the free energy barrier of 106 kJ/mol from the PMF for the 20% bilayer, we get a rate of 10^{-8} – 10^{-9} flips/s. We predict DPPC flip-flop in bilayers with 20% cholesterol to occur on a time scale of 10^8 – 10^9 s (3–30 years). For the 40% bilayer, with a free energy barrier of 111 kJ/mol the time scale would increase to 10^9 – 10^{10} s (30–300 years). Although these calculations are not rigorous, the free energy barrier for the DPPC reaching the bilayer interior will dominate the rate for flip-flop. It is apparent from the large increase in the free energy barrier that a high cholesterol content will reduce the rate of DPPC flip-flop by orders of magnitude.

Kol et al. have shown experimentally that peptide-induced flip-flop is strongly attenuated by cholesterol.¹⁰ Although this experiment involved peptides that are known to induce flip-flop (KALP23 and WALP23), the effect of cholesterol can likely be extrapolated to bilayers without peptides. The large effect of cholesterol on lipid flip-flop shown in our calculated PMFs agrees with the suggestion that the cholesterol concentration could be used as a regulatory mechanism for flip-flop along the exocytotic pathway.¹⁰ In the ER membrane, where there is a low concentration of cholesterol, flip-flop would be more prevalent, while in the plasma membrane with a high cholesterol concentration, flip-flop would be more regulated. This could help to explain the symmetric lipid distribution between leaflets in the ER and the asymmetric, highly controlled distribution observed in plasma membranes. It would be easier, and less energetically expensive, to maintain the asymmetric distribution of the plasma membrane with a high cholesterol content.

Chemical Potential. An interesting aspect of the calculated PMFs is the free energies of desorption, which are equal to the excess chemical potential of DPPC in the bilayers compared to water. We can infer the relative affinity of DPPC for the different bilayers by comparing these chemical potentials. Phase separation and lateral domain formation are important biophysical processes and are governed by chemical potential gradients. Lipids will diffuse from high to low chemical potential until reaching equilibrium or a uniform chemical potential in the system.

We find DPPC has the greatest affinity for pure DPPC bilayers and the lowest affinity for the 40% bilayer. One possible explanation for DPPC's preference for bilayers with a low cholesterol content is that, due to its conformational flexibility, restricting the movement of the tails of DPPC comes at an entropic cost. At short distances (0.5 nm) from its equilibrium position in the 40% bilayer, DPPC can fold its tails in bulk water, instead of interacting with the bilayer. This is in contrast to the 0% and 20% bilayers, where there is a clear transition at distances ~ 1.5 nm from their equilibrium position between DPPC tails interacting with the bilayer and folding up into bulk water.

Although the difference in the DPPC chemical potential between the 0% and 40% bilayers suggests a driving force for DPPC partitioning away from cholesterol and possible phase separation, without more simulations at both higher and lower cholesterol concentrations, as well as calculations of the chemical potential for cholesterol in all the bilayers, it is impossible to predict phase behavior. The large discrepancy we observe suggests DPPC and cholesterol do not mix ideally, but whether phase separation would occur is unclear. We note that it is still currently debated whether the phase diagram for cholesterol–DPPC mixtures contains a liquid-ordered–liquid-disordered coexistence region.⁵⁰ In the future, investigating the thermodynamics of lipid-phase behavior using MD simulations will be computationally feasible.

Our results show that DPPC prefers to be in bilayers with a low cholesterol content. DPPC is widely used as a model lipid in experiments, although it is not a major component of typical biological membranes. Cholesterol is known to preferentially associate with sphingomyelin compared to saturated PC lipids and has the lowest affinity for polyunsaturated PC lipids.¹¹ Repeating our calculations for more biologically relevant lipids, such as an unsaturated lipid or sphingomyelin, would be interesting.

Small Fluctuations. From the PMFs, we can extract the average distance individual DPPC molecules move within normal thermal fluctuations. Taking as a benchmark $2RT$, we measured the distance across the well of the PMF. We find that at high concentrations cholesterol impedes the fluctuations of DPPC, which is consistent with cholesterol's well-known effect of ordering and rigidifying lipid bilayers. Fluctuations of individual lipids are important for interacting with soluble enzymes, as well as lipid transfer proteins.⁵¹ The hydrophobic matching of the bilayer to accommodate integral membrane proteins has been speculated to affect protein partitioning and functioning.⁵² Collective fluctuations are involved with the elastic properties of bilayers such as the bending modulus. Consistent with our results, it was shown that the bending modulus of a DPPC bilayer increased when the cholesterol content was increased.¹⁹ We observe a thermodynamic basis for the energetic cost of small fluctuations of individual phospholipids. In bilayers with a high cholesterol content, such as the plasma membrane, phospholipids would fluctuate less than in bilayers with a low cholesterol content, such as the ER membrane.

Conclusion

We present a thermodynamic view of DPPC partitioning in lipid bilayers containing cholesterol. Our results provide insight into the ordering and condensing effects of cholesterol on individual DPPC molecules. We find cholesterol has a large effect on DPPC equilibrium stability, as well as on its extreme fluctuations from equilibrium. Additionally, we observe that cholesterol prevents the formation of water pores and defects and in general increases the free energy for the translocation of charged molecules. The 80 kJ/mol free energy barrier for DPPC flip-flop increases in bilayers containing 20 and 40 mol % cholesterol to ~ 110 kJ/mol, causing the rate of flip-flop to increase by orders of magnitude. The chemical potential of

(48) Marrink, S. J.; Lindahl, E.; Edholm, O.; Mark, A. E. *J. Am. Chem. Soc.* **2001**, *123*, 8638–9.

(49) de Vries, A. H.; Mark, A. E.; Marrink, S. J. *J. Am. Chem. Soc.* **2004**, *126*, 4488–9.

(50) Veatch, S. L.; Keller, S. L. *Biochim. Biophys. Acta* **2005**, *1746*, 172–85.

(51) Tall, A. R. *J. Lipid Res.* **1986**, *27*, 361–7.

(52) Jensen, M. O.; Mouritsen, O. G. *Biochim. Biophys. Acta* **2004**, *1666*, 205–26.

DPPC increases as the cholesterol content increases, suggesting DPPC prefers bilayers devoid of cholesterol. This work is a step forward in understanding cholesterol's role in the thermodynamics governing lipid membranes.

Acknowledgment. W.F.D.B. and J.L.M. were supported by studentships from the Natural Sciences and Engineering Research

Council (NSERC, Canada) and the Alberta Heritage Foundation for Medical Research (AHFMR). D.P.T. is an AHFMR Senior Scholar and Canadian Institutes for Health Research New Investigator. This work was supported by NSERC. Calculations were done in part on WestGrid facilities.

JA808541R